

## A NEW METHOD OF ESTIMATING REVERBERATION CHAMBER $Q$ -FACTOR WITH EXPERIMENTAL VALIDATION

Song Wang<sup>\*</sup>, Zhancheng Wu, Guanghui Wei, Yaozhong Cui, and Lisi Fan

Research Institute of Electrostatic and Electromagnetic Protection, Mechanical Engineering College, 97 Heping West Road, Shijiazhuang 050003, China

**Abstract**—Through exploring the relationship between the  $Q$ -factor and the normalized electric field strength of a reverberation chamber, this contribution proposes a new kind of methods for the  $Q$ -factor estimation, which can simplify the procedure of measuring  $Q$ -factor in experiment and raise the efficiency of calculating  $Q$ -factor by simulation. Firstly, the method is validated using measured electric field, then it is verified using data from RC's simulation by FDTD. Satisfactory agreements confirm this kind of methods could act as a reliable tool in estimating  $Q$ -factor by both experimental measurement and numerical simulation.

### 1. INTRODUCTION

The reverberation chamber (RC) is an essentially electrically large cavity made of highly reflective metallic walls and excited by a source. It has been widely used in both emission and immunity tests [1, 2]. The quality factor ( $Q$ -factor) is a parameter that indicates the cavity's ability of energy storage.  $Q$ -factor plays an important role in design and measurement of a RC, since several parameters are related to it, such as time constant,  $Q$ -bandwidth and the RC's total losses.

Over the years, many efforts have been made to derive a reasonable method for  $Q$ -factor's estimation [3–5].  $Q$ -factor calculated by the existing theoretical expression is usually much larger than actual value, because it is hard to include all kinds of losses into the expression [6]. Based on  $Q$ -factor bandwidth formula, an improved

---

*Received 7 September 2012, Accepted 1 December 2012, Scheduled 4 December 2012*

\* Corresponding author: Song Wang (wansonde@gmail.com).

method was proposed using quadratic curve-fitting technique to obtain the half-power bandwidth and  $Q$ -factor [7], but the required frequency resolution is still quite high which is not easy to satisfy. 3D full wave simulation of RC makes it possible to numerically analyze the RC's performance [8] and obtain the optimal RC's configuration [9, 10], at the same time it is a promising way to give reliable  $Q$ -factor providing there exists a precise or approached calculation expression for  $Q$ -factor. In measurement, the  $Q$ -factor is determined by measuring the average received power on receiving antenna over ensemble stirrers' rotations [11]. It is time consuming to apply this routine in RC's 3D simulation. Using cavity theory, a numerical method for  $Q$ -factor estimation of intrinsic RC was proposed [12], but it did not take advantage of time-domain simulation which is able to obtain broadband responses. Besides, the loss disposal in this method probably didn't meet the actual loss level.

Based on the definition of  $Q$ -factor, we derive another calculation expression of  $Q$ -factor and propose a simple and effective approach to calculate it. Favorable agreement is reached between the results from the proposed method and the suggested method from [11].

## 2. THEORETICAL DERIVATION OF THE NEW CALCULATION METHOD FOR $Q$ -FACTOR

The  $Q$ -factor is defined as

$$Q = \frac{\omega U}{P_d}, \quad (1)$$

where  $\omega = 2\pi f$  is the angular frequency,  $U$  the energy stored by RC, and  $P_d$  the average dissipated power in a period corresponding to  $f$ .

The energy stored in a RC is expressed as

$$U = \frac{\varepsilon}{2} \int_0^a \int_0^b \int_0^c |E|^2 dx dy dz, \quad (2)$$

where  $\varepsilon$  is the permittivity of the propagation medium, and  $a, b, c$  are the cavity dimensions in the  $x, y, z$  directions, respectively.  $|E|$  stands for the magnitude of the electric field vector.

Considering the energy-steady condition when the RC's input power  $P_{\text{inp}}$  is equal to  $P_d$

$$P_{\text{inp}} = P_d \quad (3)$$

and combining Equations (1), (2) and (3),  $Q$ -factor can be rewritten as

$$Q = \frac{\varepsilon \omega}{2} \int_0^a \int_0^b \int_0^c |\bar{E}|^2 dx dy dz \quad (4)$$

with

$$|\bar{E}| = \frac{|E|}{\sqrt{P_{\text{inp}}}} \quad (5)$$

which is called normalized electric field in the standard [11].

Considering the stirrers' rotations,  $Q$ -factor can be represented as

$$Q = \frac{\varepsilon\omega}{2} \int_0^a \int_0^b \int_0^c \langle |\bar{E}| \rangle^2 dx dy dz \quad (6)$$

where  $\langle \cdot \rangle$  indicates an average over a complete stirrer rotation cycle. This expression reveals the relationship between the  $Q$ -factor and the normalized electric field within the RC or any other reverberant cavities. It can be simplified as follows.

When a RC is equipped with a suit of efficient stirrers and is well-stirred, it is easy to meet the field uniform specified by [11] and the inside electric field environment is assumed to be spatial statistical uniform and statistical isotropic. Under this condition, it is feasible to replace the volume integral in Equation (6) by discrete summation. Firstly, a few sampling points are selected. They are well-distributed points within the RC's working volume and the electric field strength is recorded at these points. Then, the results from multiple stirrer's positions are projected to one position considering each sampling points' mean value of electric field strength over multiple stirrers' positions. Finally, the Equation (6) is approximated by

$$Q = \frac{1}{2} \varepsilon\omega V |\tilde{E}|^2 \quad (7)$$

where  $|\tilde{E}|$  is the total average of  $|\bar{E}|$  taking all the stirrer's positions and sampling points into account and  $V$  the RC's volume.

Recalling the characteristic of spatial statistical uniform, the amplitudes of  $E$ -field vary not only with the stirrer's position but also with the location of sampling point. An appropriate selection of stirrer's positions and sampling points will help the Equation (7) to give reasonable  $Q$ -factor. The numbers of selected stirrers' positions and electric field sampling points are named  $n_s$  and  $n_e$ , respectively. In measurement, confined to limited devices, it seems convenient to get  $|\tilde{E}|$  with smaller  $n_e$  and bigger  $n_s$ . Under this selection, the method based on Equation (7) is called *q<sub>e</sub>-method* whose result is labelled  $Q_E$ . In simulation, getting  $|\tilde{E}|$  with smaller  $n_s$  and bigger  $n_e$  is obviously preferred because each position requires one time simulation, and the resultant method is named *q<sub>s</sub>-method* whose result is labelled  $Q_S$ . The method represented by Equation (7) and its simplified versions *q<sub>s</sub>-method* and *q<sub>e</sub>-method* are called the new methods of calculating the  $Q$ -factor. This kind of methods is derived directly

from  $Q$ -factor's definition considering the energy-steady condition and spatial uniformity characteristic, so it can be applied to  $Q$ -factor's experimental measurement and numerical simulation.

### 3. EXPERIMENTAL VALIDATION OF THE NEW METHOD

#### 3.1. A Short Introduction of RC's Measurement Procedure

The formula for  $Q$ -factor's calculation in measurement is given by

$$Q = \frac{16\pi^2 V}{\eta_{Tx}\eta_{Rx}\lambda^3} \left\langle \frac{P_{AveRec}}{P_{inp}} \right\rangle \quad (8)$$

with

$$\left\langle \frac{P_{AveRec}}{P_{inp}} \right\rangle \quad (9)$$

representing the average rate of received power to RC's input power over one complete stirrer rotation cycle considering several receiving antenna's locations [11].  $\eta_{Tx}$  and  $\eta_{Rx}$  are antenna's efficiency factors.

The RC under test has dimensions of 10.5 m  $\times$  8.0 m  $\times$  4.3 m and it is equipped with two different stirrers. The walls and stirrers' paddles are made of galvanized steel. The fundamental resonance frequency is 23.6 MHz and the LUF (lowest usable frequency) is about 80 MHz. In measurement, the common procedure using CW excitation was adopted. The two stirrers rotated in step by step mode generating  $7 \times 7 = 49$  different positions. The input power in Watt was obtained via power meter according to (A.1) in [11]. The receiving power for all stirrers' positions at 8 different receiving antenna's locations was recorded from 80 MHz to 300 MHz with the frequency step being 2 MHz. The  $Q$ -factor was obtained by Equation (8), which is regarded as the actual value, named  $Q_M$ . Meanwhile, a cubic working volume was selected according to [11]. The 8 vertex of the working volume were chosen as 8 sampling points. For every point, electric field strength in three orthogonal directions at each stirrers' position was recorded. The normalized electric fields magnitudes were computed by Equation (5).

#### 3.2. Results of Validation

The  $Q$ -factor is calculated by Equation (7) using  $|\tilde{E}|$  computed in three different ways. Firstly,  $|\tilde{E}|$  is obtained considering all the 49 stirrers' positions and 8 sampling points and the corresponding result is labelled  $Q_{ave}$ . Then, take  $n_e = 4$  and  $n_s = 49$  to get  $Q_E$ , while using  $n_e = 8$  and  $n_s = 4$  to obtain  $Q_S$ . The comparisons of  $Q_{ave}$ ,  $Q_E$ ,  $Q_S$  and

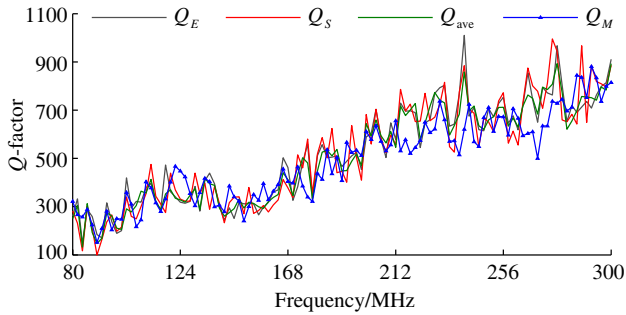


**Figure 1.** Measured  $Q_E$ ,  $Q_S$ ,  $Q_{ave}$  and  $Q_M$ .

$Q_M$  are shown in Figure 1. Obviously,  $Q$ -factor rises up with some oscillations as frequency increases. A satisfactory agreement is reached between  $Q_{ave}$  and  $Q_M$ , which proves the feasibility and effectiveness of Equation (7). When  $n_s$  or  $n_e$  is reduced significantly, the consistency only decreases slightly as embodied by  $Q_S$  or  $Q_E$ . The agreement could become better to a certain extent with the increase in  $n_s$  and  $n_e$  reflecting the enhancement of average effect in Equation (7), but the agreement reached by  $Q_S$  and  $Q_E$  is still passable and acceptable.

Moreover, 15 different sets of  $Q_E$  with  $n_e = 4$  are obtained, where the 4 electric field sampling points are chosen randomly for each set. And 15 different sets of  $Q_S$  with  $n_s = 4$  are derived similarly. We calculated the statistical mean  $\mu$  and variance  $\sigma$  for these different sets of  $Q_E$  and  $Q_S$ . From Figure 2, we can see that  $\mu$  is indeed close to  $Q_M$  and  $\sigma$  is small enough to be acceptable. In fact, the mean values of  $\sigma(Q_E)$  and  $\sigma(Q_S)$  within the investigated frequency band are 42 and 60 respectively.  $\sigma(Q_E)$  is smaller because of the uniform field within the working volume. Altogether, it is verified that reliable  $Q$ -factor can be derived using reduced stirrers' positions or sampling points by the new methods. Therefore, the proposed methods can simplify the procedure of measuring  $Q$ -factor in experiment and raise the efficiency of calculating  $Q$ -factor by simulation.

#### 4. IMPLEMENTATION OF THE NEW METHOD IN RC'S SIMULATION

In order to obtain the ensemble average, the program must be executed  $N$  times independently corresponding to the  $N$  different stirrers' positions. Therefore, it is preferred to use  $q_s$ -method.

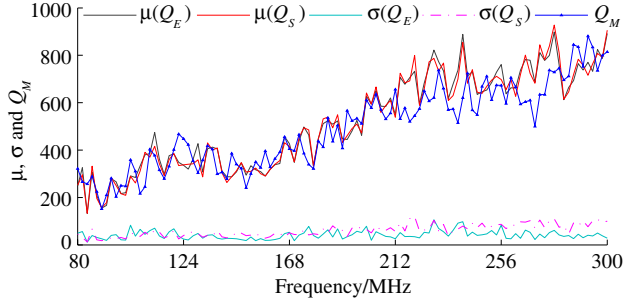


**Figure 2.**  $\mu$  and  $\sigma$  for different sets of  $Q_E$  and  $Q_S$  from measurement.

#### 4.1. Configuration of the RC's FDTD Simulation

Using FDTD, we create the RC's numerical model in which the spatial meshing step is  $dx = dy = dz = 0.1\text{ m}$  and the time step  $dt = 1.668 \times 10^{-10}\text{ s}$  meeting the CFL condition. The transiting antenna is a dipole antenna whose length is  $1.6\text{ m}$  with a  $dx$  length gap in the middle. The dipole antenna is modelled using the thin wire modelling technique and it is excited via a transmission line formulated as the same as [13]. The excitation waveform added to the transmission line is a modulated Gaussian impulse within frequency band from  $80\text{ MHz}$  to  $300\text{ MHz}$ . A working volume was chosen in the same way as measurement.

The simulation must run until the energy inside the RC is small enough, so it is important to introduce appropriate losses considering the finite conductivity of the materials or adding lossy media to save computer resources maintaining the accuracy of the results. It was found that the overall losses of a RC made by aluminium material can be approximated by setting the air's conductivity  $\sigma_{\text{air}}$  to be  $10^{-5}\text{ S/m}$  and treating the material as PEC ending up with slightly affecting the field distributions [13]. Similarly, in the case of a RC made by galvanized steel, we found its overall losses could be approximated by increasing  $\sigma_{\text{air}}$  to  $2 \times 10^{-5}\text{ S/m}$ . For other RCs made by different materials, it is only needed to adjust  $\sigma_{\text{air}}$  to an appropriate value or using another appropriate losses disposal technique.

#### 4.2. Numerical Results and Analysis

Because we emphasize the method *q<sub>s</sub>-method*, 25 stirrers' positions were simulated. Meanwhile, more electric field sampling points were set which were distributed uniformly in the working volume including the eight vertex. For each position, the simulation ran for 30000

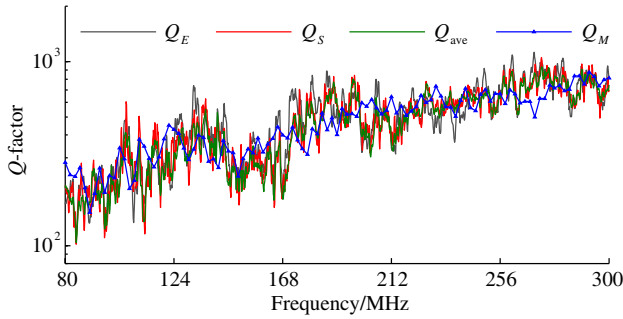


**Figure 3.** Simulated  $Q_E$ ,  $Q_S$ ,  $Q_{ave}$  and  $Q_M$ .

iterations when the amplitude of the electric field decreased below  $1/100$  of the maximum value. The frequency domain amplitude was obtained by applying FFT to the time responses of electric fields. The antenna's radiated power was evaluated considering the surface integral of Poynting flux on a virtual closed surface that just circumscribes the antenna in open space configuration. We calculated the radiated power by an additional FDTD subroutine in which the same  $dx$ ,  $dt$  and FFT were employed. This radiated power is assumed to be equal to the RC's input power  $P_{inp}$  and is used to normalize electric field according to Equation (5).

Firstly,  $Q_{ave}$  is obtained using all the stirrers' positions and sampling points.  $Q_E$  and  $Q_S$  are calculated using  $n_s = 25$ ,  $n_e = 4$  and  $n_s = 4$ ,  $n_e = 36$  respectively, where the 4 stirrers' different positions and 4 sampling points are selected randomly. Their comparisons with  $Q_M$  are shown in Figure 3. All the  $Q$ -factors rise up along with frequency. The trends of  $Q_{ave}$ ,  $Q_S$  and  $Q_E$  resemble that of  $Q_M$  quite well. Their values are close to  $Q_M$  with oscillations to a certain degree. This kind of oscillation becomes weaker slightly as  $n_s \times n_e$  goes larger, which means better average effect in Equation (7). In view of the approximation in both RC's modeling and the loss disposal, the agreement in Figure 3 could be regarded as just passable and acceptable. What's more,  $Q_S$  resembles  $Q_M$  very much, telling us it is not necessary to consider all the stirrers' positions in  $Q$ -factor's numeral evaluation.

Then,  $Q_S$  is calculated with reduced  $n_s$  being 3 and 2 while keeping  $n_e = 36$ . Their comparisons with  $Q_M$  are shown in Figure 4. As we can see, all the three  $Q_S$  share the same variation trend similar to that of  $Q_M$ . Consistent with the previous discussion, the existing oscillations turn weaker slightly as  $n_s$  goes up. Recalling Figure 3, the increase in  $n_s$  will bring little influence on the oscillations when  $n_s$  is already

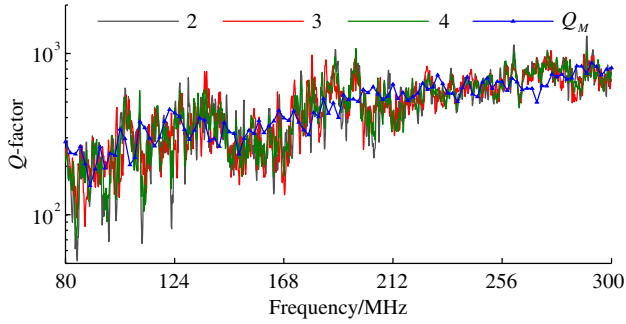


**Figure 4.** Simulated  $Q_S$  with  $n_s = 2, 3, 4$  and  $Q_M$ .

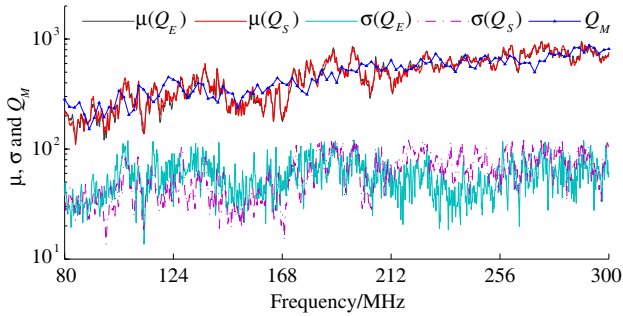


**Figure 5.**  $\mu$  and  $\sigma$  for different sets of  $Q_E$  and  $Q_S$  by simulation.

larger than 4. So using 4 stirrers' positions is feasible to get the reliable  $Q$ -factor through  $q_s$ -method. Similar to Figure 2, the  $\mu$  and  $\sigma$  for 15 different sets of  $Q_E$  and  $Q_S$  by simulation are shown in Figure 5, where  $\mu$  is close to  $Q_M$  and  $\sigma$  is acceptable (below 100 with the mean value of about 50). In short, the proposed methods are effective in estimating the  $Q$ -factor of a RC by simulation. What's more, notable computation work can be saved using  $q_s$ -method.

## 5. CONCLUSION

The relationship between the  $Q$ -factor and normalized electric field of a RC is analyzed in detail. A general expression for  $Q$ -factor is derived. Based on two simplified versions of the general expression, the methods called  $q_s$ -method and  $q_e$ -method are proposed. Using the measured electric field, a satisfactory agreement is reached between the output from  $q_s$ -method or  $q_e$ -method and the measured  $Q$ -factor. These methods are applicable to  $Q$ -factor's experimental measurement

and numerical simulation, because they are derived directly from  $Q$ -factor's definition considering the energy-steady condition and spatial uniformity characteristic.  $q_e$ -method is suitable for  $Q$ -factor's experimental measurement, since it requires fewer electric field sampling points. In RC's numerical simulation, every stirrers' position requires one time simulation. As  $q_s$ -method emphasizes on using as few as possible stirrers' positions, it is available to act as a reliable approach to obtain the approximate  $Q$ -factor by simulation. Here, we carried out the RC's FDTD simulation, but this method is applicable to RC's frequency-domain simulation as well. It is found that for a RC made of galvanized steel, its overall losses could be approximated by setting the conductivity of air to  $2 \times 10^{-5}$  S/m. Once again, passable agreements are obtained using the simulated data. What's more, 4 stirrers' positions are enough for  $q_s$ -method to obtain the  $Q$ -factor close to the measured values. Consequently, the computation time will be cut down notably compared to the expression used in experiment.

## REFERENCES

1. Mariani Primiani, V. and F. Moglie, "Numerical simulation of LOS and NLOS conditions for an antenna inside a reverberation chamber," *Journal of Electromagnetic Waves and Applications*, Vol. 24, Nos. 17–18, 2319–2331, 2010.
2. Moglie, F., V. Mariani Primiani, and A. P. Pastore, "Modeling of the human exposure inside a random plane wave field," *Progress In Electromagnetics Research B*, Vol. 29, 251–267, 2011.
3. Hill, D. A., "A reflection coefficient derivation for the  $Q$  of a reverberation chamber," *IEEE Trans. Electromagn. Compat.*, Vol. 38, No. 4, 591–592, 1996.
4. Corona, P., G. Ferrara, and M. Migliaccio, "A spectral approach for the determination of the reverberating chamber quality factor," *IEEE Trans. Electromagn. Compat.*, Vol. 40, No. 2, 145–153, 1998.
5. Arnaut, R., "Statistics of the quality factor of a rectangular reverberation chamber," *IEEE Trans. Electromagn. Compat.*, Vol. 45, No. 1, 61–76, 2003.
6. Hill, D. A., M. T. Ma, and A. R. Ondrejka, "Aperture excitation of electrically large, lossy cavities," *IEEE Trans. Electromagn. Compat.*, Vol. 34, No. 3, 169–178, 1994.
7. Robinson, M. and J. Clegg, "Improved determination of  $Q$ -factor and resonant frequency by a quadratic curve-fitting method," *IEEE Trans. Electromagn. Compat.*, Vol. 47, No. 2, 399–402, 2005.

8. Mariani, P. V. and F. Moglie, "Numerical simulation of reverberation chamber parameters affecting the received power statistics," *IEEE Trans. Electromagn. Compat.*, Vol. 54, No. 3, 522–532, 2012.
9. Hong, J.-I. and C.-S. Huh, "Optimization of stirrer with various parameters in reverberation chamber," *Progress In Electromagnetics Research*, Vol. 104, 15–30, 2010.
10. Moglie, F. and P. V. Mariani, "Numerical analysis of a new location for the working volume inside a reverberation chamber," *IEEE Trans. Electromagn. Compat.*, Vol. 54, No. 2, 238–245, 2012.
11. IEC 61000-4-21, "Electromagnetic compatibility (EMC) — Part 4-21: Testing and measurement techniques — Reverberation chamber test methods," 2011.
12. Kouveliotis, N. K., P. T. Trakadas, and C. N. Capsalis, "FDTD calculation of quality factor of vibrating intrinsic reverberation chamber," *Electronics Letters*, Vol. 38, No. 16, 861–862, 2002.
13. Moglie, F., "Convergence of the reverberation chambers to the equilibrium analyzed with the finite-difference time-domain algorithm," *IEEE Trans. Electromagn. Compat.*, Vol. 46, No. 3, 469–476, 2004.